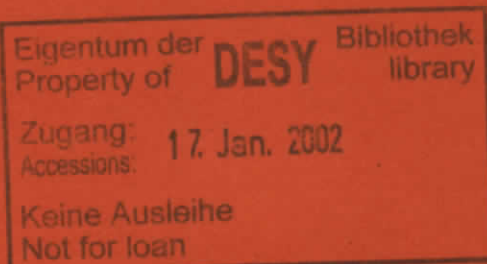


DESY SR-82-20
October 1982



PHOTOIONIZATION OF XENON BELOW THE ATOMIC IONIZATION POTENTIAL

by

P. Laporte

Equipe de Spectroscopie, C.N.R.S., Saint Etienne

V. Saile

HASYLAB, Deutsches Elektronen-Synchrotron DESY, Hamburg

R. Reininger, U. Asaf and I.T. Steinberger

Racah Institute of Physics, The Hebrew University, Jerusalem

DESY behält sich alle Rechte für den Fall der Schutzrechtserteilung und für die wirtschaftliche Verwertung der in diesem Bericht enthaltenen Informationen vor.

DESY reserves all rights for commercial use of information included in this report, especially in case of filing application for or grant of patents.

To be sure that your preprints are promptly included in the
HIGH ENERGY PHYSICS INDEX ,
send them to the following address (if possible by air mail) :

DESY
Bibliothek
Notkestrasse 85
2 Hamburg 52
Germany

DESY SR-82-20
October 1982

PHOTOIONIZATION OF XENON BELOW THE ATOMIC IONIZATION POTENTIAL

P. Laporte, Equipe de Spectroscopie, C.N.R.S. (LA 171), 158 bis cours
Fauriel, 42023 Saint Etienne, Cedex, France

V. Saile, HASYLAB, Deutsches Elektronen-Synchrotron (DESY), 2000 Hamburg
52, Federal Republic of Germany

R. Reininger, U. Asaf and I.T. Steinberger, Racah Institute of Physics,
The Hebrew University, Jerusalem, Israel

Abstract

Experiments using monochromated synchrotron radiation revealed that for densities of the order of 10^{19} atoms/cm³ and more xenon exhibits a continuous photoresponse excitation spectrum below the atomic ionization potential (12.12 eV). The lower limit of the continuum is at about 11.10 eV, the energy difference between the ground state of the molecular ion Xe₂⁺ and that of the free atom. This is attributed to the Hornbeck-Molnar process occurring at the line wings as well as at the line centres. Dips appearing in the continuum very near to positions of atomic lines are discussed invoking the quasi-static theory.

to be published in Phys. Rev. A

It has been repeatedly pointed out that liquid xenon near the triple point has electronic properties similar to that of a crystalline photoconducting insulator: the electron mobility is very high;^{1,2} there exists a rather sharp photoconduction threshold very near to the position of the threshold in the solid³; excitonic peaks as in the solid are observed in the reflection spectrum of the liquid as well^{4,5}. Following the evolution of the exciton peaks with density brings out that the peaks are distinct from atomic lines broadened and shifted by molecular interactions^{6,7}. Thus xenon can serve as a convenient model system^{8,9} for the study of the evolution of energy bands of a non-metal with the decrease of interatomic distance simply by recording the changes of the electronic properties upon gradual compression of the gas to densities nearing that of the solid.

The experiments were performed using the synchrotron radiation source in HASYLAB at the Deutsches Elektronen Synchrotron in Hamburg. The Hornormi monochromator, cryostat and data-acquisition system¹⁰ was used. The stainless steel sample cell was equipped with a LiF front window; the inner side of the window was covered by a pair of intertwined gold electrodes prepared by sputtering. The interelectrode distance was 0.36 mm; for all experiments a potential difference of 2 V was applied. Ultra-high vacuum could be achieved in the cell; the cell could also withstand pressures of up to 100 atmospheres. Temperature variations from 77^oK to 400^oK could also be obtained with the same construction. Deutsche l'Air Liquide N 47 grade xenon gas was used without further purification. The all-stainless-steel gas-handling system was baked under pumping for several hours before starting the experiments; the base

pressure in the system and in the cell was of the order of 10^{-7} torr. Before letting in the xenon gas, the system and the cell were repeatedly purged by helium at pressures of several atmospheres.

Figure 1. shows the observed photocurrent (without corrections or normalization) at a low density ($\sim 10^{-18}$ atoms/cm³) as a function of the photon energy of the incident light. The current peaks coincide in position with the respective atomic lines, but they are considerably broader. The instrumental line width at half height was about 0.02 eV. No photoresponse was seen below the 11.160 eV peak. Above the highest energy peak shown the LiF cutoff prevented further observations; in fact, even the two highest-energy peaks in Fig. 2 fall in the absorption edge region of the window and therefore their shape and height could not be rendered correctly. It is of interest to compare these results with those obtained by Huffman and Katayama¹¹. These authors measured ionization currents at number densities much lower (1 torr or less) than in our work. All lines observed by these authors and situated at photon energies $h\nu < 11.85$ eV were seen in the course of the present work as well (Fig. 2), though somewhat broadened. The hierarchy of intensities is also similar for the two works. Because of the general broadening, the two neighbouring lines associated with the $9s[1\frac{1}{2}]^0$ and $5d'[1\frac{1}{2}]^0$ levels are not resolved in Fig. 2, though they are distinct in Ref. 11; the same is true about the two levels $8d[1\frac{1}{2}]^0$ and $10s[1\frac{1}{2}]^0$. The transitions to the levels $9d[0\frac{1}{2}]^0$ (11.801eV) and $9d[1\frac{1}{2}]^0$ (11.835 eV) were not observed in Ref. 11, since the intensity of the argon continuum source employed by Huffman and Katayama was zero in this spectral region.

The use of a closed cell in the present work (see also Ref. 12) made possible to study the influence of increasing density on the photoionization excitation spectrum. The photoresponse, as presented in Fig. 2, was obtained from the photoelectric current measured at 2 volts by normalization to equal number of incident photons and division by the electron mobility. For the normalization, the relative number of photons passing through the LiF window was measured as a function of photon energy. Division by the zero-field electron mobility² was necessary in order to separate the density-dependence of the mobility from the density-dependence of the carrier concentration. Figure 2 presents the photoresponse at four densities at room temperature, corresponding to a pressure range of about 50 millibar to 40 barr. The graphs were selected from an extensive series covering this density range in such a manner as to emphasize the qualitative changes. Note that for $h\nu > 11.7$ eV the spectrum refers to a strongly absorbing region of the lithium fluoride window, thus the correction for the absorption is large and therefore no quantitative conclusions should be drawn from the graphs in this region.

When comparing the four graphs of Fig. 2 the following points stand out:

a. The lowest-density graph exhibits peaks; in the next one presented the peaks become dips on a slowly varying background. With increasing the density further, the dips shift to lower photon energies, broaden and eventually wash out.

b. The photoresponse for $\rho_N \sim 10^{18} \text{ cm}^{-3}$ is smaller than that at the higher densities by an order of magnitude. However, for the other three densities not only the order of magnitude stays the same, but, if the minima are disregarded, the spectra can be fitted with envelopes of roughly similar shapes and heights (ignoring, as suggested above, the region $h\nu > 11.7 \text{ eV}$).

c. The envelopes of the three higher-density graphs drop sharply on the low-energy side. The position of this threshold shifts slightly with increasing density to lower photon energies: from 11.16 eV for $\rho_N = 0.41 \times 10^{20} \text{ atoms/cm}^3$ to 11.11 eV at the highest density presented.

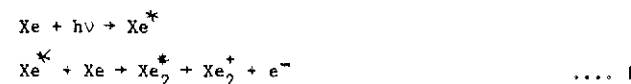
d. For the three spectra corresponding to the higher densities there is a low-energy tail beyond the drop mentioned in "c". With increasing density this tail appears already at lower photon energies and its contribution to the photoresponse at the position of the drop becomes more and more significant. At still higher densities, reported separately¹³ this tail becomes the dominant feature of the spectrum.

Figure 3 shows the photon energies of the various peaks and the respective dips as a function of the number density. It is seen that the general trend is a slight shift to lower photon energies with increasing density. Simultaneously the dips become broader and shallower, as demonstrated in Fig. 2.

For the discussion of the mechanism underlying the reported effects it is useful to note again that the envelope of the photoresponse continuum (above $\sim 11.1 \text{ eV}$) changes little with density in a wide range,

though for the same density range the low-energy tail changes markedly. At densities above those discussed here¹³ this tail can be shown to be due to photoconductivity proper, namely to excitations into a quasi-free state (conduction band), the position of which is determined by the average interaction of thermal or nearly-thermal electrons with the medium. Therefore one is naturally led to the assumption that, in contrast with the effects in the tail, most of the response at the densities in question is due to photoionization and governed by atomic or molecular interactions.

It was seen in Figure 1 that at the lowest densities photoresponse appears at the positions of atomic absorption lines, for photon energies well below the ionization energy (12.12 eV) of the free xenon atom. As in Ref. 11, the response is attributed to photoionization via the Hornbeck-Molnar process¹⁴. In this process an excited atom Xe interacts with a ground state atom forming a molecular ion and a free electron:



Direct ionization of Xe_2 in supersonic beams showed^{15,16} that for these processes to take place there is no need for collision with a further Xe atom. For these processes the photon energy $h\nu$ must conform with the inequality

$$I_G(\text{Xe}) - D(\text{Xe}_2^+) \leq h\nu \leq I_G(\text{Xe}) \quad \dots 2$$

where $I_G(\text{Xe})$ represents the ionization energy of the xenon atom and $D(\text{Xe}_2^+)$ the dissociation energy of the xenon molecular ion. The very small kinetic energies and the negligible energy of the vibrational ground state of Xe_2^+ were ignored in the above considerations. The threshold energy can be calculated as

$$I_G(\text{Xe}) - D(\text{Xe}_2^+) = I_G(\text{Xe}_2) - D(\text{Xe}_2) \quad \dots 3$$

where $I_G(\text{Xe}_2)$ is adiabatic ionization potential and $D(\text{Xe}_2)$ the dissociation energy of the van der Waals molecule Xe_2 . Substituting numerical values from the work of Dehmer and Dehmer¹⁵ into Eq. 3 we obtain for the threshold energy the value of 11.10 eV. On the other hand Figure 2 shows that the photoresponse continuum sets in at 11.11 to 11.16 eV, depending on the density, in good agreement with the above threshold. This fact suggests that all photoresponse in the continuum whether at the atomic lines or not, should be attributed to the Hornbeck-Molnar process. Such a generalization of the Hornbeck-Molnar process for a continuum of photon energies also follows from considering the theory relevant at the densities in question to the absorption line wings, namely the nearest-neighbour quasi-static approximation. According to this approximation, there is a one-to-one correspondence between the frequency ν at each point of the wing of an absorption line and the distance r of the excited atom to its nearest neighbour, the exact functional relationship between r and ν being given by the details of the configurational energy diagram. It is nevertheless clear that decreasing ν on the low-frequency side of the absorption line implies excitation of atoms with lower values of r

along the potential curve representing attraction between the excited atom and its nearest neighbour. One may assume that smaller r implies less probability of the excimer to decay by channels other than the formation of the molecular ion and concurrent liberation of an electron. It follows that the red wing of an absorption line can make a considerable contribution to the Hornbeck-Molnar process. This fact, along with the above comparison of the energy thresholds, leads to the realization that the photoionization response by means of the Hornbeck-Molnar process at an atomic absorption line should manifest as a rather broad band, especially at higher densities. The overlap of a set of neighbouring bands creates the continuous absorption seen in Fig. 2. This is the central result of the present study.

One of the most striking features of Fig. 2 is the appearance of inverted peaks at higher densities. At first sight it is tempting to attribute the observed inversion to the dependence of the lifetime of the liberated electrons on the penetration depth of the incident radiation. Accordingly the penetration depth $d = 1/\alpha$ (α being the absorption coefficient) at the line centre ν_0 of a self-broadened line is very small ($\sim 10 \text{ nm}$)¹⁷, thus for the centre the lifetime might considerably be shortened due to recombination at the Xe-LiF interface or by energy transfer effects. On the other hand such surface effects would not shorten the lifetime for the wings where the penetration depth is larger. Thus at the wings the lifetime could be appreciably longer than at the centre, resulting to an inversion of the line. In the density range involved d either stays constant at the line centre or even decreases somewhat with density while it increases with density in the wings¹⁷.

Even if it stays constant, decreasing of the density would imply simply an overall narrowing of the photoresponse profile, thus, except for a narrowing, a similar response would be obtained at low densities as at a high one in contrast with experiment. If, on the other hand, d for excitation at the line centre decreases with increasing density the conflict with experiment is even sharper, since this would imply that low densities favour line inversion and not high ones.

The most likely explanation for the lineshape inversion is based on considering the competition between electron liberation via the Hornbeck-Molnar process and all other decay channels. According to the above discussion, increase of $\nu_0 - \nu$ implies transition with a smaller nearest-neighbour distance r . Therefore the Hornbeck-Molnar process becomes more dominant the higher the pressure and the larger the value $\nu_0 - \nu$. In other words, an inversion of the lineshape may occur with increasing density.

The fact that the dips corresponding to atomic lines become broader and shallower at high densities can also be understood on the basis of the variations of the profile of absorption line: with increasing density the absorption line profiles broader and flatten simultaneously and cause broadening of the photoresponse profile with simultaneous flattening of the dips. The red-shift of the dips and of the onset with increasing density are at least partly due to the usual effect of attractive potentials, including many-body effects, especially at higher densities. One of these effects is expressed by the polarization energy P^+ of the hole left in the dense medium after removal of

the electron. For the density range involved P^+ has been calculated¹³ to increase from zero to 0.04 eV. This is nearly equal to the observed shift (Fig. 2) of the onset of the Hornbeck-Molnar effect with density. It should also be noted that the sense of variation of the onset is in full accord with the expected enhancement of the photoresponse at the line wings with density. The shift of the dips is markedly larger than expected from the values of P^+ alone.

The Hornbeck-Molnar process as observed for a continuum of photon energies in the present work, is an interesting novel way of creating free electrons in a dense gas and its possible influence should be taken into account under appropriate conditions, especially when studying the spectroscopy and dynamics of excimers.

Acknowledgments

The authors wish to express their thanks to several institutions (DESY, DAAD and the Israel Commission for Basic Research) and numerous individuals for their contributions towards the success of this work.

References

1. L.S. Miller, S. Howe and W.E. Spear, Phys. Rev. 166, 871 (1968).
2. S.S.S. Huang and G.R. Freeman, J. Chem. Phys. 68(4), 1355 (1978).
3. U. Asaf and I.T. Steinberger, Phys. Rev. B10, 4464 (1974).
4. D. Beaglehole, Phys. Rev. Lett. 15, 551 (1965).
5. I.T. Steinberger and U. Asaf, Phys. Rev. B8, 914 (1973).
6. P. Laporte and I.T. Steinberger, Phys. Rev. A15, 2538 (1977).
7. P. Laporte, J.L. Subtil, U. Asaf, I.T. Steinberger and S. Wind, Phys. Rev. Lett. 45, 2138 (1980).
8. R. Reininger, U. Asaf, P. Laporte and I.T. Steinberger, in Proceedings of the Seventh International Conference on Conduction and Breakdown in Dielectric Liquids, Berlin, 1981, edited by W.F. Schmidt, Berlin, 1981, p. 69; J. of Electrostatics 12, 123 (1982).
9. R. Reininger, U. Asaf and I.T. Steinberger, Chem. Phys. Letters, in press
10. V. Saile, P. Görtler, E.E. Koch, A. Kozevnikov, M. Skibowski and W. Steinmann, Appl. Opt. 15, 2559 (1976).
11. R.E. Huffman and D.H. Katayama, J. Chem. Phys. 45, 138 (1966).
12. J.A.R. Samson and R.B. Cairns, J. Opt. Soc. Am. 56, 1140 (1966).
13. R. Reininger, U. Asaf, I.T. Steinberger, V. Saile and P. Laporte submitted to Phys. Rev. B15
14. J.A. Hornbeck and J.P. Molnar, Phys. Rev. 84, 621 (1951).
15. P.M. Dehmer and J.L. Dehmer, J. Chem. Phys. 68(8), 3462 (1978).
16. C.Y. Ng, D.J. Trevor, B.H. Mohan and Y.T. Lee, J. Chem. Phys. 65, 4327 (1976)
17. P. Laporte and H. Damany, J. Phys. (Paris) 40, 9 (1979).

Figure Captions

- Fig. 1 Photocurrent as a function of photon energy for $\rho_N = 10^{18}$ atoms/cm³.
- Fig. 2 Photocurrent normalized for equal number of incident photons and divided by the zero-field mobility as a function of the photon energy, at four densities. The spectra were taken at room temperature.
- Fig. 3 The density-dependence of the position of the peaks (open circles) and dips (full circles) corresponding to six atomic transitions.

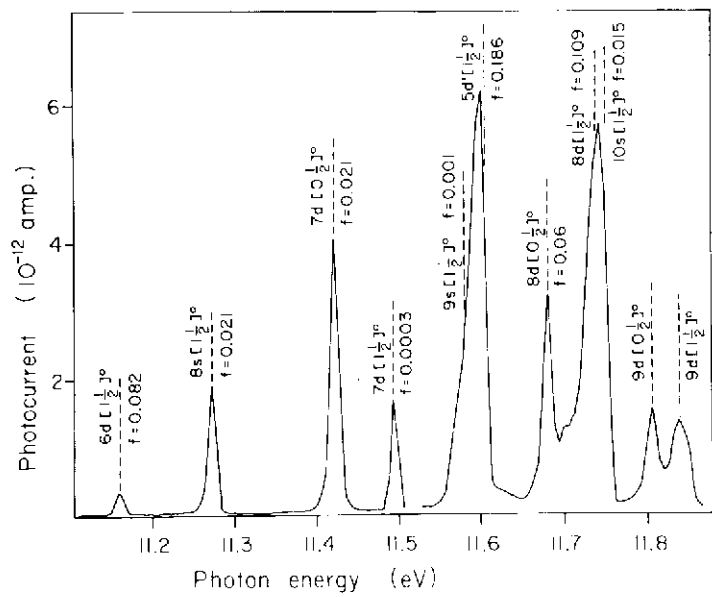


Fig. 1

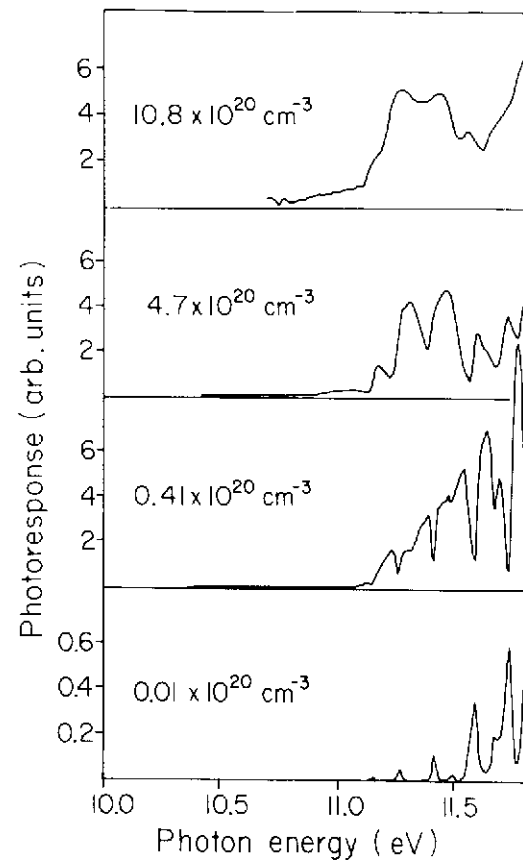


Fig. 2

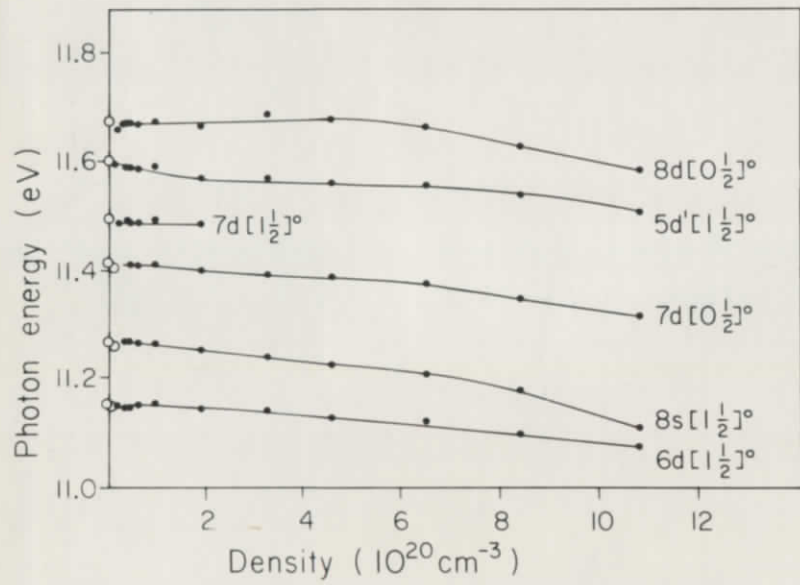


Fig. 3